NEW DEVELOPMENTS IN FRACTURE TOUGHNESS EVALUATION

W. Schmitt*, W. Böhme*, D.-Z. Sun*

Micromechanical material models are applied to analyse ductile failure processes during tensile tests and Charpy-V tests. The parameters are used to predict J-resistance curves for neutron-embrittled weld material of nuclear pressure vessels. To validate the approach, dynamic tensile tests and instrumented impact tests with notched and precracked Charpy specimens are performed and simulated. The results suggest that the critical void volume fraction f_c and the characteristic length l_c are practically independent of strain-rate and specimen geometry. The tunnelling of the crack in the interior of the Charpy specimen is predicted in a satisfactory way by a three-dimensional analysis with a strain-rate dependent Gurson model.

INTRODUCTION

The safety evaluation of nuclear reactor components based on fracture mechanics concepts requires the determination of fracture toughness data or resistance curves from laboratory specimens. The size requirements for valid tests and the limited capacities of irradiation surveillance capsules do not allow to monitor toughness degradation, e.g. as a consequence of neutron flux directly by means of standard fracture mechanics testing.

Compared with conventional fracture mechanics concepts, micromechanical models have the advantage that the corresponding material parameters for ductile fracture can be transferred between different specimen geometries and over a large size scale. Another advantage is that studies of material failure with those models can lead to a better understanding of rupture processes, especially for nonhomogeneous materials, and thus help to optimize material toughness. Two models based on a flow function derived by Gurson (1) and modified by Needleman and Tvergaard (2,3) were applied to analyse the damage behaviour

*Fraunhofer-Institut für Werkstoffmechanik, Freiburg, Germany

of smooth and notched bars as well as of Charpy-V specimens and used to predict the onset of crack growth in cracked specimens. The description of ductile rupture processes, void nucleation, growth and coalescence, is incorporated in the constitutive relations. The applicability of this model was verified by Sun et al. (4,5) by using parameters determined from smooth tensile tests to predict not only the results of notched bar tests but also ductile crack initiation and extension in various types of precracked specimens using an additional length parameter.

Since the variation of strain-rate influences both the material flow behaviour and the fracture processes, two questions have to be answered before a micromechanical model is used for dynamic loading. First, which material model does appropriately describe the effects of the strain-rate hardening, including the thermally softening effects? Second, do the micromechanical parameters depend on strain-rate, and how can they be determined? To solve the problems, a theoretical and an empirical strain-rate dependent material model, both based on the modified Gurson flow function were implemented in a commercial finite-element program. Static and dynamic tensile tests and instrumented impact tests with Charpy-V and SEN(B) specimens were carried out.

STRAIN-RATE DEPENDENT GURSON MODELS

One of the models was developed by Macherauch and Vöhringer (6) and describes the strain-rate dependency of the flow stress based on thermal activation processes. This model is denoted by model 1 and the details about its parameters may be found in (7). Another applied model (model 2) was introduced by Pan et al. (8):

$$\sigma = \sigma_G(\varepsilon, T_o)\,[1-\beta(T-T_o)]\left(\frac{\dot{\varepsilon}_p}{\dot{\varepsilon}_o}\right)^m \quad , \quad m << 1 \quad (\textit{model 2}) \qquad (1)$$

$\dot{\varepsilon}_o$ and T_o are a reference strain-rate and a reference temperature, respectively, and σ_G denotes the flow stress measured at $\dot{\varepsilon}_o$ and T_o. β is a material dependent parameter. During plastic deformation nearly all plastic work is converted into heat. At high strain- rates the heat transfer during deformation is negligible and the temperature elevation can be calculated from the dissipated plastic work. The adiabatic heating results in a softening of the material due to the reduction of the yield stress. This effect has been considered in both material models.

Both strain-rate dependent models have been combined with the modified Gurson model (3,9) which is based on a plastic potential applicable to porous

solids:

$$\Phi = \frac{3\sigma'_{ij}\,\sigma'_{ij}}{2\sigma^2} + 2q_1 f^* \cosh\left(\frac{\sigma_{kk}}{2\sigma}\right) - [1 + (q_1 f^*)^2] = 0 \qquad (2)$$

σ denotes the flow stress of the matrix material, which depends on strain, strain-rate and temperature. f^* is a function of the void volume fraction, f, and was suggested by Needleman and Tvergaard (2) to simulate the rapid loss in stress carrying capacity of the material caused by void coalescence. In the modified Gurson model initiation and propagation of the crack are a natural result of the local softening due to the void coalescence, which begins when a critical void volume fraction f_c is exceeded over a characteristic distance l_c (5).

The parameters for the modified Gurson model, except the f_c-value, were taken from reference (3) and a previous study (5). For the ferritic pressure vessel steel 22 NiMoCr 3 7 (≈ ASTM A 508 Cl 2) at room temperature the critical void fraction f_c = 0.045 was determined by fitting the sudden drop in the measured load vs. diameter change curve of static tensile test with the calculated one. It was assumed that the material is initially void free. The void fraction at fracture was taken to be f_f = 0.2.

APPLICATION TO INSTRUMENTED CHARPY-V TESTS

Since the Charpy-V-notch impact tests are more frequently used than dynamic tensile tests or fracture mechanics tests, it is desirable to determine the material parameters for the strain-rate dependent models directly from the Charpy-V test. To achieve these goals, experimental and numerical tools and procedures had to be refined and developed further in several aspects, among them:

- the experimental determination of dynamic stress-strain curves up to failure strain and the consideration of strain-rate dependent flow properties in numerical calculations in combination with damage models
- the proper numerical treatment of the contact and friction problem arising during the Charpy test
- three-dimensional finite element models to consider the variation in constraint between the central-plane and the free surface of a Charpy specimen and the corresponding variation in the damage behaviour

Strain-Rate Dependent Material Behaviour

The strain-rate dependent material behaviour of the steel 22 NiMoCr 3 7 was determined in static and dynamic experiments with smooth tensile specimens at room temperature. The diameter and the measure length of the tensile bars are

6 mm and 30 mm respectively. During the static tensile tests with a servohydraulic testing machine the strain-rate was $\dot{\varepsilon} = 2 \cdot 10^{-4}$/s. The dynamic tests were performed in a drop weight tower with an impacting mass of 273 kg. At impact velocities of 2 to 4 m/s initial strain-rates of $\dot{\varepsilon} = 50$ to 100/s were achieved. For the evaluation of true stress vs. true strain curves the specimens were photographed during the impact tests with a 24-spark Cranz-Schardin high speed camera. From the photographs elongation, area reduction and necking radius were measured (10).

For small deformations the measured dynamic loads are significantly higher than the static ones. With increasing deformation the static and dynamic curves fall together. This effect can be partly explained by adiabatic softening, which is negligible up to the maximum load and mainly occurring in the necking part of the dynamic tensile specimens. The load vs. diameter-change curve measured in the dynamic tensile tests can be well predicted by taking into account the adiabatic softening with the parameter $\beta = 0.0008$/K, which is however twice the value $\beta = 0.0004$/K evaluated from the static yield stresses measured at 293 K and 493 K. Similar results were obtained using model 1. These results indicate that the adiabatic softening is probably not the only reason for the reduction of the dynamic flow stress with increasing plastic deformation.

The material parameters describing the strain-rate hardening were evaluated from numerical simulations of the tensile tests. For model 2 the parameter $m = 0.0175$ was obtained by inserting the stresses at maximum load and the corresponding strain-rates into equation (1). The final rupture of the dynamic tensile specimens can be predicted in a satisfactory way with the micromechanical parameters used for the simulation of the static tests, if the plastic deformation behaviour of the specimen is well modelled. This means that the critical damage parameter f_c is practically independent of strain-rate (10).

Contact And Friction Problems

The complex loading situation of the Charpy tests including sliding and friction at the anvils makes the numerical simulation more difficult. Therefore, some experiments were performed with additional instrumentation of the Charpy specimen, as sketched in Fig. 1, to study the behaviour at the supports in more detail (10). An acceptable solution was found by modelling the supports of the specimen with contact surfaces and the hammer with gap elements (7).

Three-Dimensional Finite Element Simulation

It is one problem for the simulation of Charpy tests, that the stress state of Charpy-specimens cannot be approximated by a two-dimensional model due to the absence of side grooves. The results of different simulations with 2D- and

combined 2D/3D-simulations are demonstrated in Fig. 2. The most accurate results were, of course, obtained by 3D-calculations.

Fig. 3 displays a three-dimensional view of the deformed near-notch mesh on which the damage zone ($f \geq f_f$) is marked. Comparison with the fracture surface of a Charpy-V specimen shows that the tunnelling of the crack in the interior of the specimen and the side contraction are well predicted.

After these developments it was possible to analyse the Charpy-V test very accurately and the micromechanical material parameters were determined by fitting the numerically calculated load curves to the measured ones. Finally, these material values were used for numerical simulations to predict J-resistance curves for dynamically loaded SEN(B) 10/10 specimens (width = 10mm / thickness = 10mm) and statically loaded CT 25 specimens. The acceptable agreement with the measured J_R-curves was demonstrated in (7).

Although both the J-integral concept and the micromechanical models can be used to analyse the ductile crack extension for the applied specimen geometries, the parameters for the micromechanical models are also applicable for different geometries of specimens or components and loading conditions. More results of this study with unirradiated material may be found in (7,10). In the following, the determination of the micromechanical toughness parameters of the irradiated RPV-material from a subsized tension bar test and directly from the record of a Charpy test will be presented.

EVALUATION OF THE IRRADIATED RPV WELD MATERIAL

The Charpy energies of the irradiated weld material for different temperatures are shown in Fig. 4. One test at T = 100 °C in the upper transition regime was selected for the evaluation and is marked. From the broken halves of this specimen subsized tensile specimens were machined as sketched in Fig. 5. A static tension test with such a subsized smooth round bar (diameter 2.6 mm) was performed by SIEMENS also at T = 100 °C. From the measured load signal of this test (see Fig. 6) the static stress-strain curve was determined and, by fitting the sudden load drop in the load vs. diameter-change curve, also the critical volume fraction of voids was calculated.

A combined plane strain - plane stress model with stress-strain curve and micromechanical parameters determined from the static tension test was then used for the simulation of the Charpy test. The strain-rate sensitivity of the material was obtained by fitting the calculated loads in the Charpy test to the measured loads up to initiation prior to maximum load.

The evaluated set of micromechanical parameters was then used to calculate the behaviour of a CT 20 compact specimen and, hence, to predict a static J-resistance curve. This static R-curve in Fig. 7 was further supported by three dynamic tests with SEN(B) 10/10 specimens fabricated (in compound technique) and tested in a 300 J pendulum by SIEMENS. These tests were performed with reduced impact energy (below 10 J) and the ductile crack growth was measured on the fracture surfaces. One test was simulated numerically; the resulting dynamic J_R-curve is also given in Fig. 7. As expected from previous studies the dynamic curve lies well above the static one. The fairly good agreement with the three experimentally determined crack-resistance data supports the calculation.

The initiation values of the static and dynamic resistance curves were formally converted into K_{Ji}-values. Since the chosen Charpy test marks the onset of the upper shelf, the results obtained at 100°C are used to adjust the ASME-K_{Ic}-curve. Thus, a reference temperature of 56°C is determined. In the adjusted position the ASME-K_{Ic}-curve is a conservative envelope of the K_{Ic}-curve of the irradiated weld material (11).

It was assumed during these investigations, that the processes of ductile crack extension are controlled by both the critical void volume fraction f_c and the characteristic length l_c, which are related physically to a micro-structural scale of a material. However, it is not easy to introduce the concept of the characteristic length into micromechanical modelling, because usual constitutive equations are formulated only for single points in a material. Moreover, the Gurson-type models show a pronounced strain-localization caused by material softening, which intensifies the well-known mesh-size dependency of numerical results, especially in the case of cracked specimen. The simple and practical method is based on the selection of a particular mesh size at the crack tip by matching the computed load vs. displacement curve with the experimental one of a cracked specimen. The results presented here were achieved by using this method. It is a disadvantage of this method, that due to complicated numerical effects the selected element size is not easily identified with the physical parameter l_c.

An alternative method is based on the introduction of a localization limiter into the constitutive equations (12). It is the basic idea of these so-called "nonlocal" models, that the evolution of the internal variables, in this case the void volume fraction f, in a given material point does not only depend on the current values of state variables in this very point, but also on the values in the vicinity of the point. The influence of neighbouring points is limited by a weighting function, which is decreasing with the distance. The parameter l_c as used in the weighting function determines the size of a region, where the increases of internal variables are averaged with the weighting function and physically characterizes micro-structural features. Several publications demonstrated the ability of this concept to reduce the mesh-sensitivity of numerical

results. The effects of a localisation limiter on the softening processes in the Gurson model will be in detail presented in (13). Fig. 8 compares the distribution of void volume fraction and the plastic deformation at the crack tip calculated using a localisation limiter (Fig. 8a) with those simulated without considering a localisation limiter (Fig. 8b). It can be recognized that the distribution of the void volume fraction computed by the "nonlocal" model is more homogeneous and reasonable.

CONCLUSIONS

Different specimen geometries and loading rates were used to study the applicability of a strain-rate dependent Gurson model to the analysis of the deformation and fracture behaviour of an unirradiated, ferritic pressure vessel steel. The results prove that the material parameters relevant for the micromechanical model can be determined likewise from the simulations of a static or a dynamic tension test or from a Charpy-V impact test. The material parameters are sufficiently independent of strain-rate and J-resistance curves can be well predicted using the micromechanical model.

Following the validation program an irradiated weld material was evaluated by testing and modelling subsized smooth tension and Charpy-type specimens. The material parameters for the simulations were abstracted from tension and Charpy-V tests. With these parameters it was possible to calculate the behaviour of CT and SEN(B) specimens and, hence, to deduce static and dynamic crack resistance curves. Furthermore, an ASME-reference curve was adjusted based on the fracture toughness determined at T = 100°C to approximate the K_{Ic}(T)-curve of the irradiated weld material.

The use of very small tension specimens raises the question of the minimum specimen size required for the evaluation of meaningful and transferable material damage parameters. Also unavoidable modification of the material properties as a consequence of the fabrication process in particular near the surface might become important. These problems need to be looked into in the frame of future research activities.

REFERENCES

(1) Gurson, A. L., J. of Engng. Materials and Techn., Vol. 99, 1977, pp. 2-15.

(2) Needleman, A. and Tvergaard, V., J. of Mechanics and Physics of Solids, Vol. 32, 1984, pp. 461-490.

(3) Needleman, A. and Tvergaard, V., J. of Mechanics and Physics of Solids, Vol. 35, 1987, pp. 151-183.

(4) Sun, D.-Z., Siegele, D., Voss, B. and Schmitt, W., Fatigue & Fracture of Engineering for Materials & Structures, Vol. 12, 1988, pp. 201-212.

(5) Sun, D.-Z., Kienzler, R., Voss, B. and Schmitt, W., "Application of Micromechanical Models to the Prediction of Ductile Fracture," Fracture Mechanics: 22. Symp. (Vol. II), ASTM STP 1131, Eds.: S. N. Atluri et al., American Soc. for Testing and Materials, Philadelphia, 1992, pp. 368-378.

(6) Macherauch, E., Vöhringer, O., Zeitschrift für Werkstofftechnik, Vol. 9, 1978, pp. 370-391.

(7) Sun, D.-Z., Hönig, A., Böhme, W., Schmitt, W., "Application of Micromechanical Models to the Analysis of Ductile Fracture under Dynamic Loading," Fracture Mechanics: 25th Volume, ASTM STP 1220, Eds.: F. Erdogan and Ronald J. Hartranft, to be published.

(8) Pan, J., Saje, M., Needleman, A., Int. J. Fracture, Vol. 21, 1983, pp. 261-278.

(9) Needleman, A., Tvergaard, V., Int. J. Fracture, Vol. 49, 1991, pp. 41-67.

(10) Böhme, W., Sun, D.-Z., Schmitt, W., Hönig, A.: Application of Micromechanical Material Models to the Evaluation of Charpy Tests, ASME-Symposium, Adv. in Local Fracture/Damage Models, Scottsdale, Arizona, April 28 - May 1, 1992, Eds.: J. H. Giovanola and A. J. Rosakis, AMD-Vol. 137, Book No. H00741, 1992, pp. 203-216

(11) Schmitt, W., Sun, D.-Z., Böhme, W., Blauel, J. G., Nagel, G.: Evaluation of Fracture Toughness from Small Specimens, Trans. 12th Int. Conf. Struct. Mech. in Reactor Techn., SMiRT 12, Stuttgart, 15-20 Aug. 1993, Ed.: K. Kussmaul, Elsevier Science Publ. B.V., Vol. G 15/2, pp. 201-206, 1993

(12) Bažant, Z., Pijaudier-Cabot, Gilles, Journal of Applied Mechanics, Vol. 55, 1988, pp. 287-293.

(13) Sun, D.-Z., Hönig, A., "Significance of the Characteristic Length for Micromechanical Modelling of Ductile Fracture," to be published, Third International Conference Localized Damage 94, Udine, Italy, 21-23, June 1994

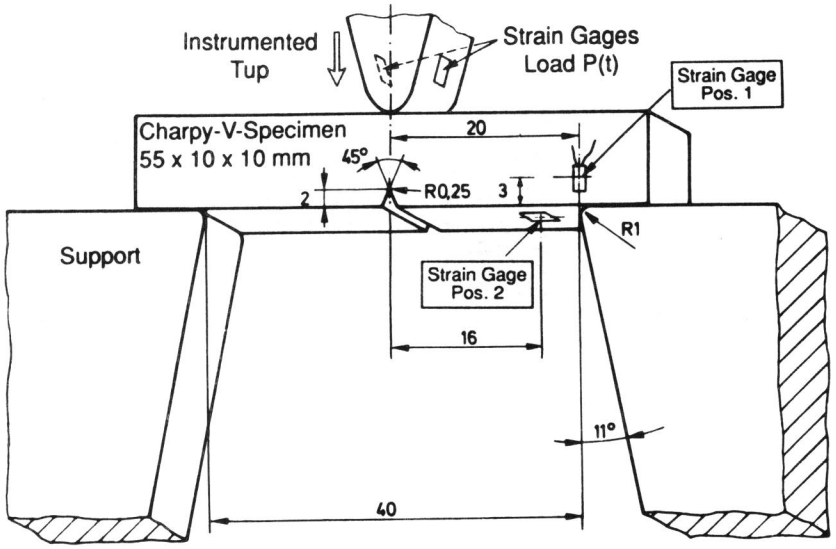

Fig. 1: Charpy specimen with additional instrumentation at the supports

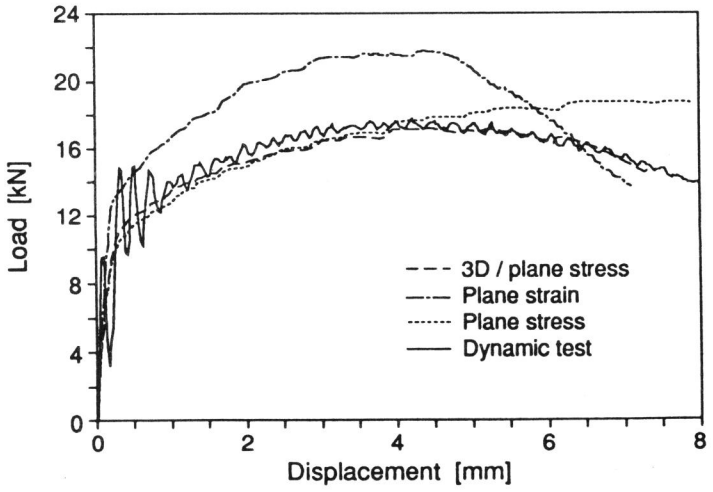

Fig. 2: Measured and calculated load-displacement curves
(different FE-models)

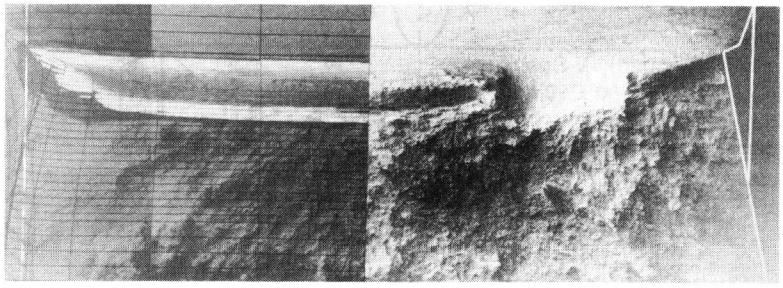

Fig. 3: Observed and calculated deformation and crack extension (Charpy-V)

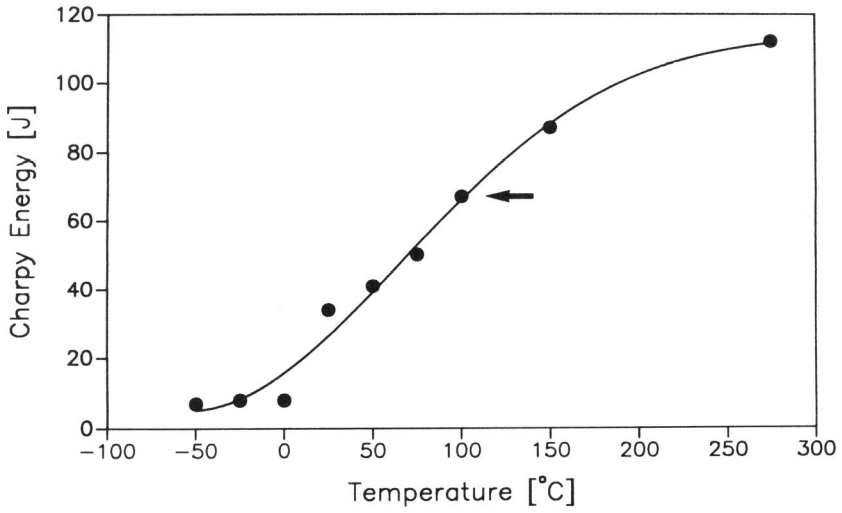

Fig. 4: Impact-energy vs. temperature of irradiated RPV weld material

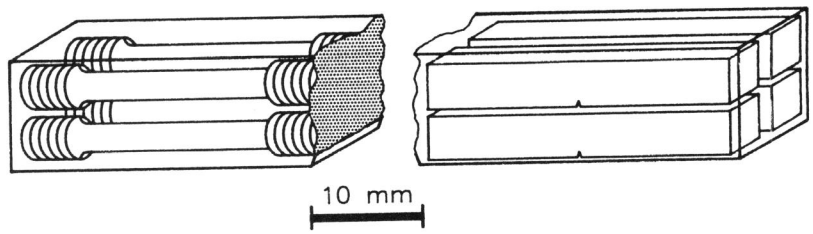

Fig. 5: Preparation of subsized specimens from broken Charpy-V specimens

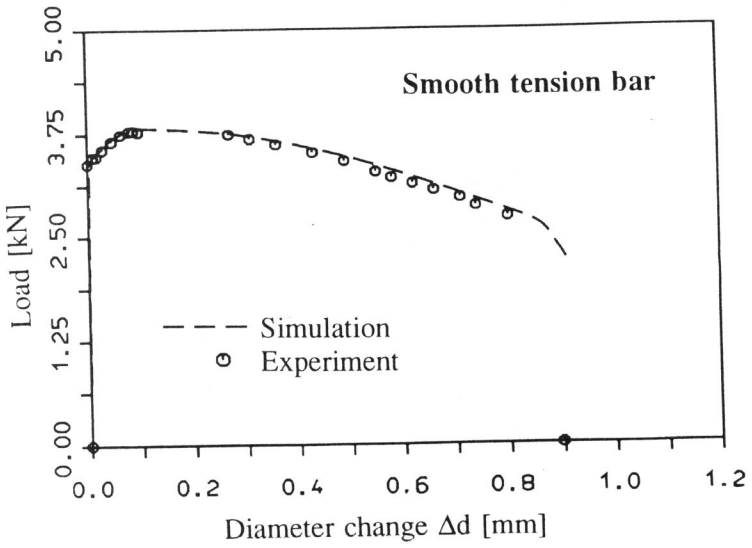

Fig. 6: Measured and calculated load for irradiated subsized tensile specimen

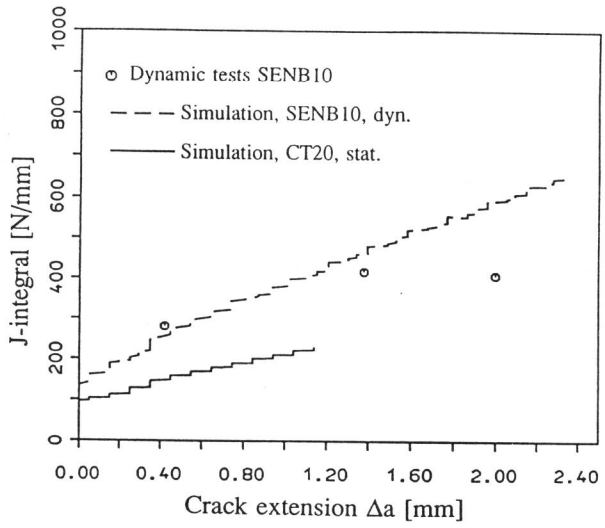

Fig. 7: Static and dynamic J-resistance curves (irradiated material)

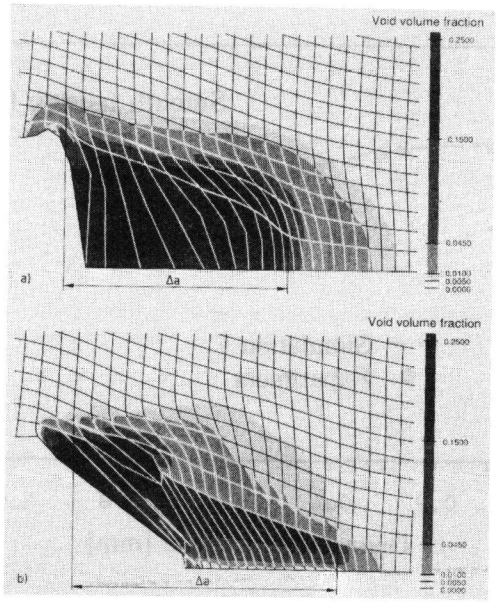

Fig. 8: Calculated damage-zones: a) with b) without localisation limiter